JOURNAL OF SPACECRAFT AND ROCKETS
Vol. 39, No. 2, March–April 2002

Earth Impact Studies for Mars Sample Return

Edwin L. Fasanella* and Yvonne Jones†
NASA Langley Research Center, Hampton, Virginia 23681-2199
and
Norman F. Knight Jr.‡ and Sotiris Kellas§
Veridian Systems, Fairfax, Virginia 22030-7305

Dynamic finite element modeling of a series of penetrometer drop tests into soft clay that were conducted as part of the Mars sample return advanced technology program is discussed. Structural impacts into soil continue to challenge analysts to develop accurate soil material models for finite element simulations to predict the observed deceleration pulse and impact crater. Parametric studies are presented for penetrometers of varying diameter, mass, and impact velocity to a maximum of 45 m/s, which is the expected terminal velocity of a sample return capsule. Parameters influencing the simulation such as the contact penalty factor and the material model representing the soil are discussed. An empirical relationship between peak deceleration and key parameters is developed and is shown to correlate experimental and analytical results. The results provide preliminary design guidelines for Earth impact that may be useful for future space exploration sample return missions.

Nomenclature

A_p = peak acceleration, g
D = diameter of penetrometer, m
E = Young's modulus, Pa
EH = hardening modulus, Pa
g = ratio of acceleration divided by acceleration of gravity, nondimensional
M = mass of penetrometer, kg
V = impact velocity, m/s
α = empirical constant, kgs^2/m^3
δ = density, kg/m^3
ν = Poisson's ratio, nondimensional
σ_y = yield stress, Pa

Introduction

FUTURE space science missions will involve the acquisition, storage, and return of sample material collected during space flight or planetary exploration.[1,2] These sample return missions may require the design of reliable Earth entry vehicles. Currently, different configurations are being studied for such vehicles with the design requirement to survive a terminal velocity impact with selected areas of the Earth's surface without the aid of a parachute. Developing an understanding of this impact scenario will provide added robustness to the vehicle design and increased reliability of the system.[3,4]

An advanced technology test program has been developed to meet this challenge. The program has provided important test results for the overall vehicle design, which can also be used for validating analytical simulation tools.[5] The optimal surface for an Earth impact of an entry vehicle carrying space exploration samples is soft soil. Thus, as part of the technology development program, low-velocity penetrometer drop tests were performed in November 1998 at the Utah Test and Training Range (UTTR) into soft clay from a bucket truck and from a hot-air balloon. Also, a series of drop tests was performed from a helicopter onto soil at impact velocities up to 45 m/s at UTTR in September 2000. These hemispherical penetrometers of varying diameter were dropped to provide impact deceleration time-history data for a range of design parameters to support sample return missions. Some limited penetration and soil sampling data from the late 1960s for low-velocity Earth impact into soft clay are also available in Refs. 6 and 7. The impact data and soil analysis in Ref. 6 were for the UTTR site but focused on long slender impactors with deep penetrations.

The objective of this paper is to describe the development of the soil impact simulation and the correlation between the numerical results and the penetrometer test data. This paper will present the drop test data, a brief description of the dynamic finite element code MSC.Dytran,[8] the discretization for the penetrometer and soil models, the soil constitutive model, contact modeling parameters, penetrometer size and velocity effects, and a comparison of test results with analysis. In addition, an empirical relationship is developed to predict the peak deceleration based on penetrometer size, mass, and impact velocity. MSC.Dytran was used to simulate these drop tests and to predict additional results when test data were not available.

Drop Test Data

Data from penetrometer drop tests conducted at UTTR from a bucket truck and from a hot-air balloon in 1998 as well as data from a helicopter drop in 2000 are summarized in Table 1. Each penetrometer is hemispherical shaped with an internal high-speed (>100k samples/s) digital data acquisition system to record the acceleration–time history. Penetrometers with diameters ranging from 0.203 to 0.66 m were used with impact velocities ranging from 5.74 to 45 m/s. The total penetrometer mass varied from 2.98 to 24.5 kg. A posttest photograph of the 0.408-m penetrometer after a 45 m/s impact at UTTR in September 2000 is shown in Fig. 1. The photograph illustrates the impact crater created in the clay lakebed.

Finite Element Modeling

The software program MSC.Dytran was used to perform the impact analysis. MSC.Dytran is an explicit, nonlinear, transient-dynamic finite element computer code with its origins related to the public-domain DYNA3D code developed at Lawrence Livermore National Laboratory. These nonlinear dynamic codes have been used extensively over the last 20 years as increased computer power has cut the solution time to hours instead of days for many problems. Although these codes are highly complex, analysts have verified the codes for a wide variety of impact problems for materials, such as

Received 13 March 2001; revision received 3 August 2001; accepted for publication 18 August 2001.

*Aerospace Engineer, U.S. Army Research Laboratory–Vehicle Technology Directorate, MS 495. Associate Fellow AIAA.
†Engineering Cooperative Education Student, University of Tennessee, MS 495. Student Member AIAA.
‡Staff Scientist, Systems Engineering Sector, Aerospace Engineering Group, 10560 Arrowhead Drive. Associate Fellow AIAA.
§Principal Engineer, Systems Engineering Sector, Aerospace Engineering Group, 10560 Arrowhead Drive.

Table 1 Test matrix of penetrometer drops at UTTR

Test	Description	Diameter, m	Mass, kg	Velocity, m/s	Peak acceleration, g
1	Drop hammer	0.203	2.98	5.74	85
2	Helicopter	0.408	12.05	34.97	1195
3	Helicopter	0.408	12.05	43.15	1482
4	Helicopter	0.408	12.05	44.9	1656
5	Helicopter	0.408	24.5	31.94	614
6	Helicopter	0.408	24.5	39.42	812
7	Helicopter	0.408	24.5	45.35	1016
8	Bucket truck	0.514	11.02	16.7	500
9	Bucket truck	0.514	18.54	19.1	300
10	Bucket truck	0.514	18.91	16.7	210
11	Balloon	0.514	18.91	21.8	325
12	Balloon	0.514	18.91	25.9	510
13	Helicopter	0.66	24.0	35	1080
14	Helicopter	0.66	24.0	40	1295

Fig. 1 Posttest photograph of 0.408-m penetrometer after a 45-m/s impact (September 2000 at UTTR).

metals, that are well behaved. The input format for MSC.Dytran was made to be as compatible as practical with MSC.Nastran, a structural analysis code widely used in the aerospace community. MSC.Dytran offers a library of structural elements (beams, shells, and solids) for modeling complex structures. MSC.Dytran also offers a variety of constitutive models for elastic, elastoplastic, and layered orthotropic materials and for crushable foams and soils, thereby allowing most engineering material systems to be analyzed. Several modeling options are available for contact, impact, and penetration including breakable joints and element erosion. Automatic time-step control is provided once the user defines an acceptable initial time step. Archive files for postprocessing data into deformed shapes and time history files to generate xy plots of selected grid points, material variables, or contact variables can be requested by the user. A restart capability for continuing the solution in time is also available.

Discretization

The finite element model of the penetrometer and soil is shown in Fig. 2. The penetrometer consists of a thick aluminum shell with internal ribs to make it relatively rigid. In the simulations, the penetrometer is represented as a rigid body with a given mass and initial impact velocity. To represent the geometry accurately, the rigid-body hemispherical penetrometer was discretized into a fine mesh of 1200 shell elements.

The soil is modeled as a hexagonal-shaped region with dimensions of approximately five times the penetrometer radius on each side. A relatively large soil domain was chosen to reduce the effects of the finite soil boundaries. The spatial discretization provides a graded mesh with smaller elements near the top-center surface where the impact will occur. The graded mesh is generated by using the two-way bias mesh seed of MSC.Patran with an element side length in the top-center region that is five times smaller than those at the bounding surfaces. There are 33 elements of varying size along the length of each side of the soil model. In the full model, the soil

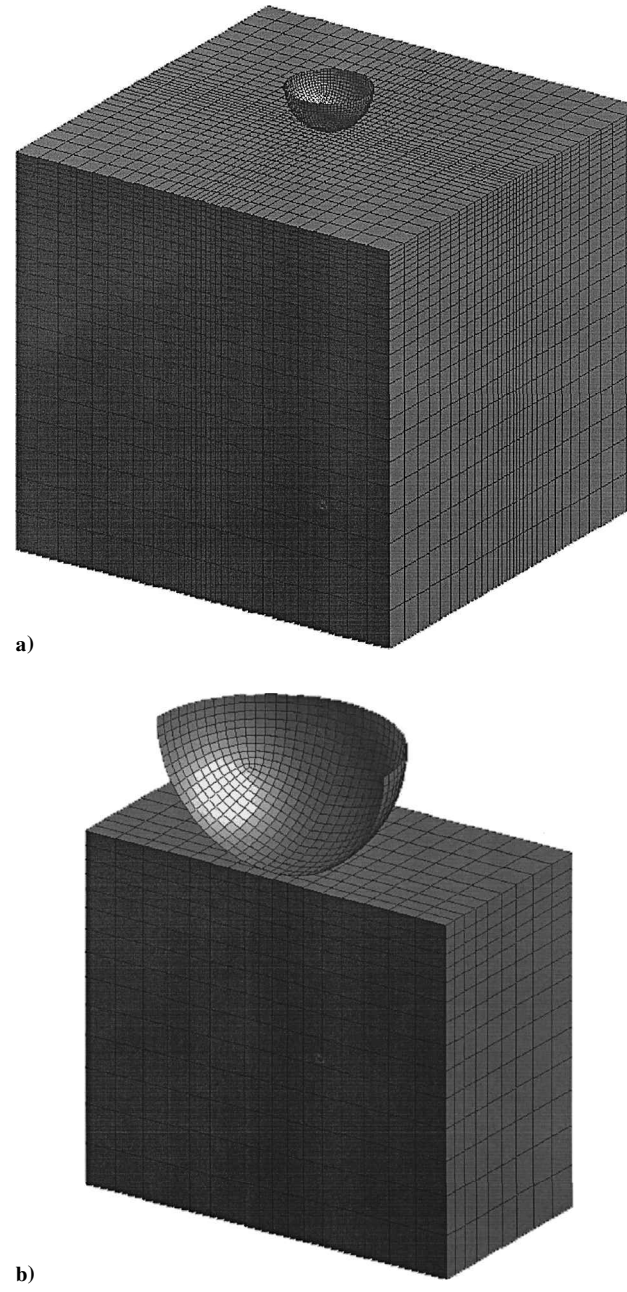

Fig. 2 Penetrometer/soil finite element: a) full model and b) closeup section of model.

is discretized into 27,225 eight-node solid single-integration-point elements. The nodes on the outer vertical surfaces of the soil are allowed to be free, whereas the nodes on the bottom surface are fully restrained. The total number of nodes in the model including both the soil and penetrometer is 31,380. In the vertical direction, the soil model is divided into two layers. The top layer is approximately one-fifth of a penetrometer radius deep, and the bottom layer consists of the rest of the soil. This division of the soil layer is included in the model because the properties of the top layer of soil could differ significantly from the deeper soil. This approach was used to represent the soil at UTTR, which is typically characterized by a dry upper layer, while the lower layer may be saturated with water.

Soil Constitutive Model

The soil was modeled as an elastic–plastic material with strain hardening (DYMAT24). The nominal values used to characterize the soil were an elastic secant modulus $E = 4000$ kPa, Poisson's ratio $\nu = 0.3$, a yield stress (or bearing pressure) $\sigma_y = 68.9$ kPa, and mass density $\delta = 2201.6$ kg/m^3 based on a 65% moisture content. A hardening modulus EH of 800 kPa ($0.2E$) was used in the final

model. Soil near the surface is estimated to have moisture content of approximately 22% during dry conditions. This soil model is an approximation to the actual soil properties and was obtained by using the charts in Ref. 6 and from information obtained by using soft clay surrogates in the laboratory.

The simple elastic–plastic material model of the soil was quite successful in predicting the UTTR test acceleration pulses and was recommended in Refs. 9 and 10. Improved correlation was obtained with the portion of the experimental acceleration pulse after the peak by including strain hardening. More complex material models for the soil such as the cap model[11] were also considered. However, the coefficients and parameters needed for the cap model could not be determined given the available data.

Contact Modeling

Contact between the rigid-body penetrometer and the soil is modeled by using the penalty method with the bounding top surface of the soil serving as the master contact surface. The nodes on the rigid penetrometer were defined as the slave nodes. Note that contact between a rigid body and a deformable body can cause numerical difficulties. However, the use of a rigid body may speed up the analysis by an order of magnitude. Generally, a master contact surface can be coarsely discretized. However, because the master surface (soil surface) deforms significantly, the discretization of the master surface is quite important for this problem. Thus, the master surface mesh in the contact zone must be much finer than for a nondeforming surface.

Some of the other contact parameters in MSC.Dytran include the type of contact (VERSION), the weighting factor (WEIGHT), the selection of the monitoring side (SIDE), and the contact penalty factor (FACT). The results presented in this paper used VERSION = V4, WEIGHT = SLAVE, and SIDE = BOTH.

The parameter FACT is quite important because it represents a scale factor for the contact force. When a slave node penetrates the master surface too deeply, the contact can be made stiffer by increasing FACT. However, for dissimilar materials with significantly differing stiffnesses, even the default value of FACT (0.1) may lead to a large contact force that may artificially overaccelerate the less dense material. Such a result could cause a separation between the slave node and master surface until the slave nodes catch up to the master surface again. Monitoring the position of adjacent nodes on the master surface and corresponding slave nodes aids in identifying this numerical artifact of the contact simulation. If the separation distance becomes too large, the value of FACT may be reduced to decrease the likelihood of excess separation between the contact surfaces.

Results and Discussion

Selected penetrometer drop tests into clay were simulated before the drop tests, and later the analytical results were correlated with the corresponding test data from UTTR. The matrix of drop tests is shown in Table 1. A Unix workstation performed the simulations by using MSC. Dytran version 2000. A typical simulation was executed for 0.025 s of actual time by using a maximum time step of 10 μs, which required about one CPU hour.

Soil Discretization and Contact Penalty Factor

The discretization of the soil beneath the penetrometer, that is, in the contact zone, and the contact penalty factor are both critical in achieving meaningful analytical results. If the soil is discretized too coarsely in the contact zone and/or the contact penalty factor is too large, the resulting graph of the penetrometer acceleration may look like a series of spikes. When the contact force is too large,

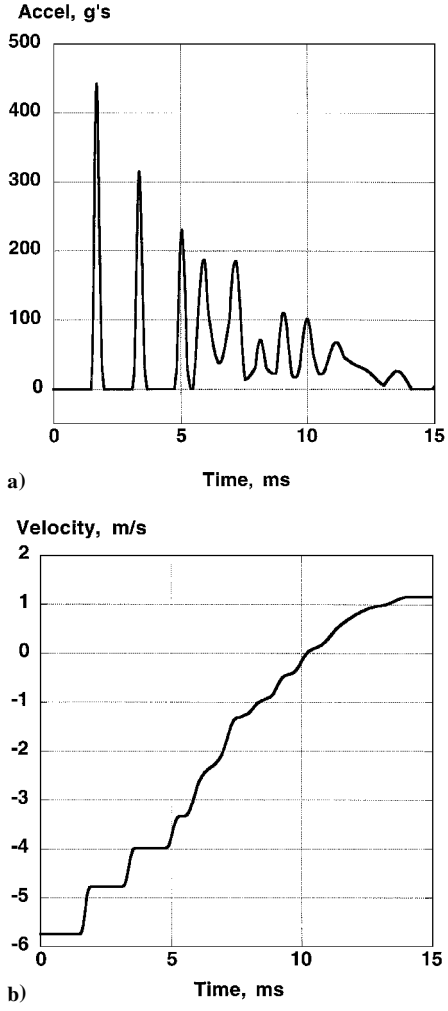

Fig. 3 Coarse contact zone model using FACT = 0.1: a) acceleration–time history and b) velocity–time history.

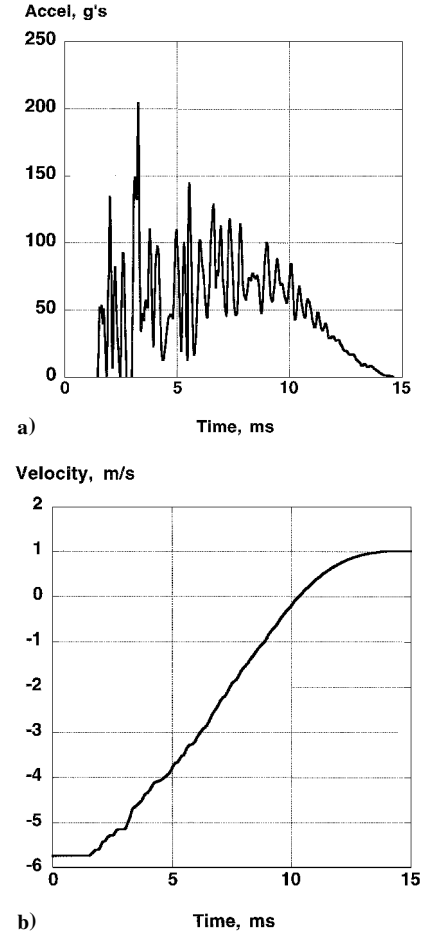

Fig. 4 Refined contact zone model using FACT = 0.1: a) acceleration–time history and b) velocity–time history.

the soil is accelerated ahead of the penetrometer. Each time the penetrometer catches up with the soil, another acceleration spike occurs. Using the default penalty factor (FACT), the contact zone mesh discretization was varied to determine its effect. The results for a 0.2-m-diam, 2.98-kg penetrometer with an impact velocity of 5.74 m/s are shown in Fig. 3. For the results in Figs. 3a and 3b, the master surface mesh beneath the sphere was coarse, with only 25 element faces in the contact zone directly beneath the penetrometer. The acceleration response of the penetrometer shown in Fig. 3a is a series of spikes, and the velocity response in Fig. 3b resembles a monotonically increasing step function. This response illustrates the repeated contact and separation that occurs because of an excessive contact force.

A refined model of the soil with approximately 120 elements in the contact zone was also analyzed to determine the effect of contact zone discretization. Results shown in Fig. 4 for the refined contact zone model differ significantly from those in Fig. 3. The stair-step behavior in the velocity–time history is replaced with a smooth curve. However, the acceleration response exhibits high peaks and high-frequency oscillations superimposed on the basic acceleration pulse.

The effect of the contact penalty factor (FACT) on the acceleration–time and velocity–time histories for the coarse and refined contact zone models is shown in Figs. 5 and 6, respectively. The response is now more characteristic of a penetration transient response. Changing the value of FACT to 0.001 is needed because of the large difference in stiffness between the penetrometer (rigid) and the soil (very weak). The acceleration–time histories shown in Figs. 5a and 6a are similar; hence, subsequent simulations use FACT = 0.001 and contact zone refinement. All velocity–time histories in Figs. 3–5 exhibit a direction change at approximately 10 m/s and a final rebound velocity of 1 m/s.

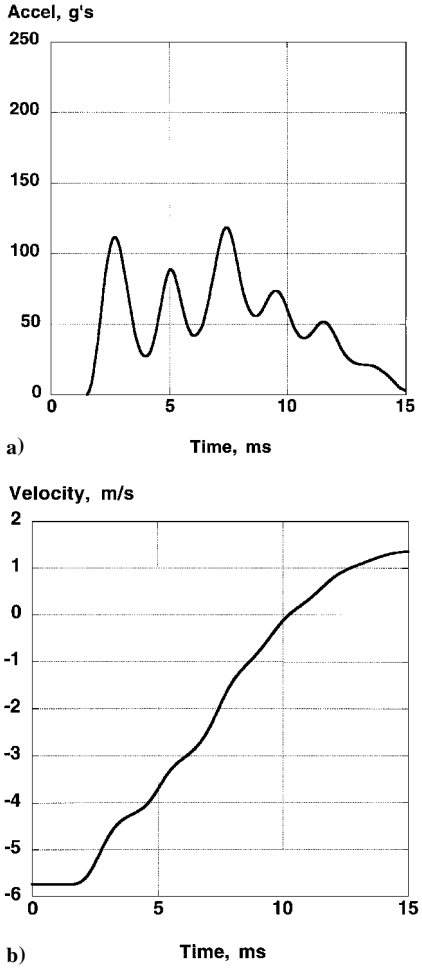

Fig. 5 Coarse contact zone model using FACT = 0.001: a) acceleration–time history and b) velocity–time history.

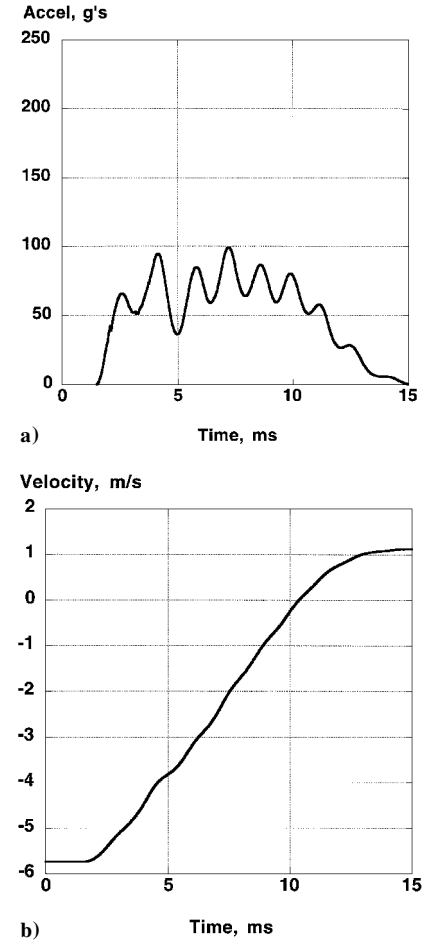

Fig. 6 Refined contact zone model using FACT = 0.001: a) acceleration–time history and b) velocity–time history.

Penetrometer Size and Velocity Effects

Next, a larger diameter penetrometer with a higher impact velocity was studied. The impact and penetration event for the 0.408-m-diam penetrometer with a mass of 12 kg and an initial velocity of 35 m/s can also be used to illustrate the effects of altering the contact penalty factor FACT in MSC.Dytran. The simulation was executed for 15 ms of real time by using a maximum time step of 10 μs. The soil model for this case and the remainder of the simulations has 27,225 eight-node solid brick elements with a single integration point. The contact zone for this case has approximately 80 element faces beneath the sphere. The rigid penetrometer is again discretized with 1200 four-node shell elements to represent the surface contour accurately. For the acceleration–time histories shown in Fig. 7, the default value of 0.1 was first used for the contact penalty factor. However, adjacent nodes on the penetrometer and soil were found to move apart rather than stay in contact. When the contact factor was reduced to 0.001, the node at the bottom of the sphere and an adjacent node of soil were found to move together, and the resulting rigid-body penetrometer acceleration response is smoothed without requiring digital filtering.

Effect of Soil Material Model

When the elastic perfectly plastic model was used, soil material parameters were varied to determine the effects on the acceleration pulse. If either the elastic modulus or the yield stress (bearing pressure) of the soil were varied by 20%, the influence on the resulting acceleration pulse was minimal. However, the effect of lowering the soil density by 20% from the nominal value reduced the peak acceleration by approximately 20%, as shown in Fig. 8. Thus, the density of the soil is an important factor in the simulation. Drier soil, like that found in the top layer at UTTR, is less dense than the bottom layers of soil, which may be saturated with water.

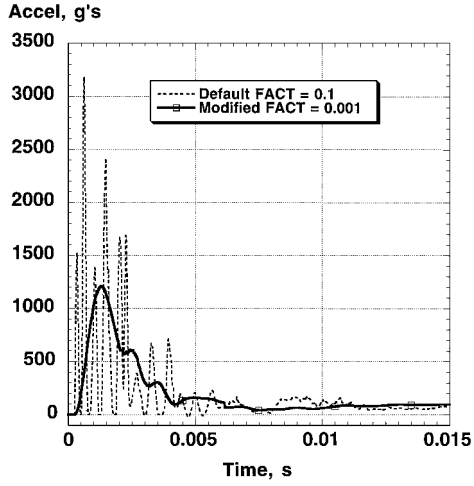

Fig. 7 Effect of penalty factor (FACT) on acceleration–time history of penetrometer.

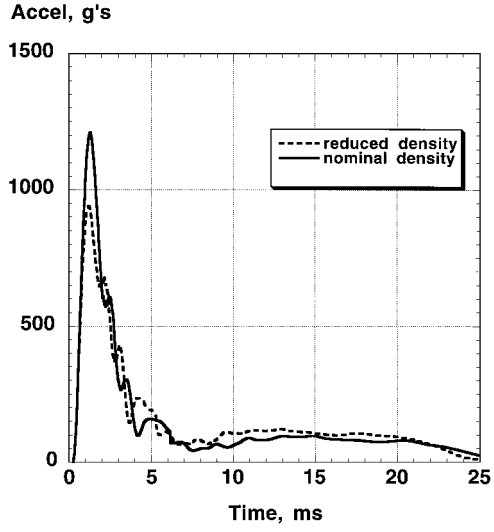

Fig. 8 Effect of clay density on peak acceleration for 0.408-m penetrometer with 12-kg total mass and impact velocity of 35 m/s.

The acceleration response in Fig. 8 for a 0.408-m-diam penetrometer weighing 12 kg with an impact velocity of 35 m/s was a pretest prediction. The acceleration peak (1200 g) for the nominal density matched the test data very well, but the dropoff of the acceleration after the peak was too sharp when compared with the test data. The pretest soil model was elastic perfectly plastic. As is evident in Fig. 9, when a hardening modulus EH equal to 20% of E was added to the material model, the peak value was not changed, but the acceleration dropoff matched the test data more closely. The hardening modulus is needed to approximate the compaction of the soil. The experimental acceleration response shown in Fig. 9 was integrated to obtain velocity and penetration depth. The predicted penetration depth, shown in Fig. 9b, compared well with the experimental value. Before the hardening modulus was introduced to simulate soil compaction, the analytical penetration was too deep.

Comparisons of Test with Analysis

Additional comparisons between test and analysis (with and without strain hardening) are shown in Figs. 10–12. The predicted acceleration peaks match the experimental data quite well and generally are within 10–15% of the experimental values. The pulse shape and duration are also simulated quite well, especially when strain hardening is included. These results indicate that the peak acceleration for a penetrometer of fixed size and mass increases as the initial impact velocity increases. For a fixed initial impact velocity, the peak acceleration increases with size (diameter) and decreases for larger masses.

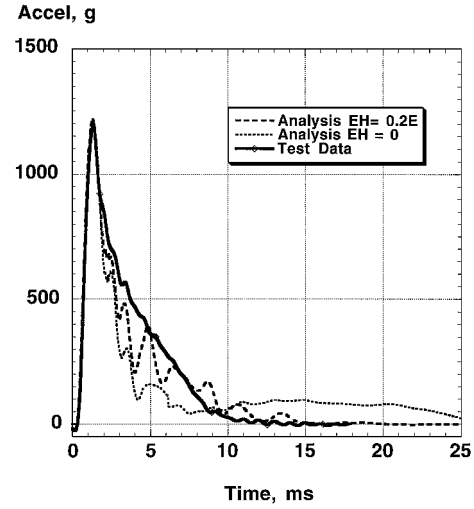

Fig. 9a Comparison of test with predicted acceleration pulse for the 0.408-m penetrometer with 12-kg total mass and impact velocity of 35 m/s.

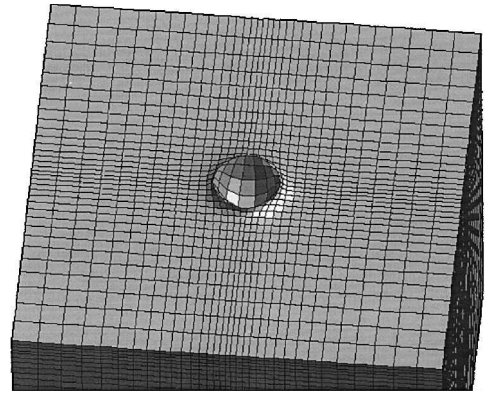

Fig. 9b Crater shown in soil model.

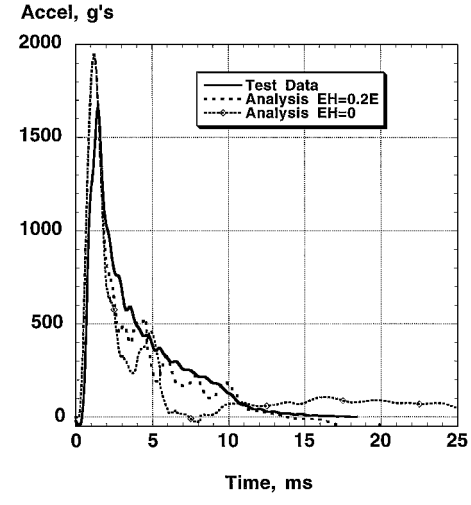

Fig. 10 Comparison of test with analysis for the 0.408-m penetrometer with 12-kg total mass and impact velocity of 45 m/s.

Empirical Relationship for Peak Acceleration

Based on test results and analysis, it was deduced that the peak acceleration was likely to be proportional to the product of the penetrometer diameter and the square of the initial impact velocity divided by the total penetrometer mass. Thus, the maximum acceleration in gravitational units g was plotted vs $\alpha DV^2/M$, where

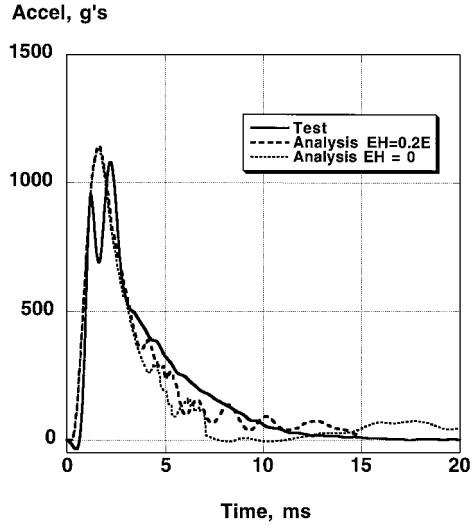

Fig. 11 Comparison of test with predicted acceleration pulse for the 0.66-m penetrometer with 24-kg total mass and impact velocity of 35 m/s.

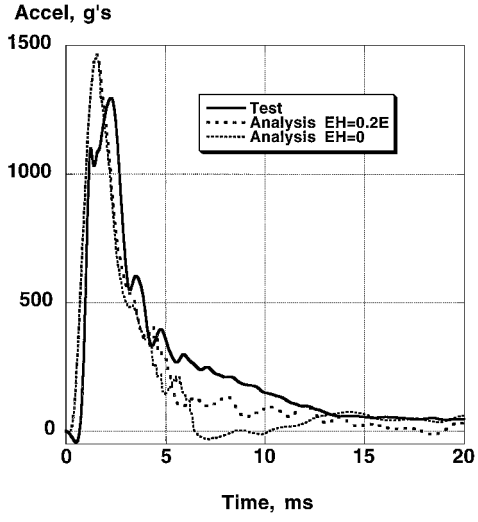

Fig. 12 Comparison of test with predicted acceleration pulse for the 0.66-m penetrometer with 24-kg total mass and impact velocity of 40 m/s.

D is the diameter of the penetrometer in meters, V is the velocity in meters per second, M is the total mass of the penetrometer in kilograms, and α is an empirical constant to be determined. Thus, the peak acceleration in the test data follows the empirical relation

$$A_p = \alpha D V^2 / M \tag{1}$$

This empirical relationship can be useful in conceptual design studies to estimate peak accelerations for soft-clay impacts. Consistent results for test and analysis were obtained over a wide range of values, including penetrometer size, mass, and initial impact velocity. These acceleration estimates should be conservative because the analytical results are based on a rigid penetrometer, whereas the actual vehicle may include energy-absorbing structure in the design.

In Fig. 13, both the experimental and analytical peak accelerations are plotted vs DV^2/M. Linear curve fits were made to both the test and analytical data and are shown in Fig. 13. The slope of the test data gives $\alpha = 27$, although the slope of the analytical data is slightly higher at 29. The results show good agreement between test and analysis for these drops into clay. If the density of the soil were lowered, the analysis would be expected to match the experimental data even better.

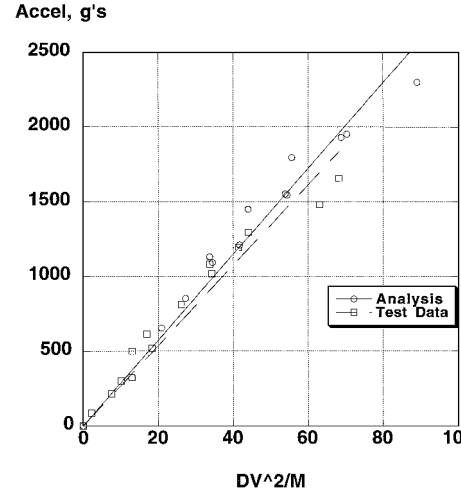

Fig. 13 Peak acceleration of penetrometer test data and analysis plotted against DV^2/M (linear fit to each set of data is shown).

Conclusions

The ideal surface for terminal-velocity Earth impact of future space exploration sample-return-mission vehicles is soft clay. Thus, to characterize the expected impact response, a series of penetrometer drop tests into soft clay was performed as part of the Mars sample return advanced technology program at the UTTR with different penetrometer sizes, masses, and impact speeds.

Pretest predictions of the peak acceleration for the tests were made with the nonlinear transient dynamic finite element code MSC.Dytran. The predicted peak accelerations that were obtained by using an elastic perfectly plastic material model for the soil were within 10–15% of the test data. However, the predicted acceleration–time history dropped off too quickly after the peak. By the addition of a 20% hardening modulus to the soil material model to represent compaction, the pulse after the peak was simulated more accurately. Consistent results for test and analysis were obtained over a wide range of values including penetrometer size, mass, and initial impact velocity.

In the analytical model, the master contact surface was defined to be the top surface of the soil, and the slave nodes were defined to be the nodes forming the rigid penetrometer. The MSC.Dytran results were found to be sensitive to the mesh discretization in the contact zone and to the contact penalty factor. The best results were obtained by reducing the contact penalty factor by two orders of magnitude from the default value (from 0.1 to 0.001).

The peak accelerations for the drops of different sized penetrometers with different masses and differing impact velocities were found to vary linearly with DV^2/M, where D is the penetrometer diameter, V is the impact velocity, and M is the penetrometer mass. This empirical relation should be useful in conceptual design studies to estimate peak accelerations.

Acknowledgments

The work performed by the last two authors was sponsored by NASA Langley Research Center under General Services Administration Contract GS-35F-4503G, Task 1418. The authors wish to thank Robert A. Mitcheltree and Stephen J. Hughes of NASA Langley Research Center for the penetrometer test data and support. This support is gratefully acknowledged.

References

[1]Mitcheltree, R. A., Bruan, R. D., Simonsen, L. C., and Hughes, S. J., "Earth Entry Vehicles for Mars Sample Return," International Astronautical Federation, Paper IAF-00-Q.3.04, Oct. 2000.

[2]Desai, P. N., Mitcheltree, R. A., and Cheatwood, F. M., "Sample Returns Missions in the Coming Decade," International Astronautical Federation, Paper IAF-00-Q.2.04, Oct. 2000.

[3]Hermann, R. J., and Lineberger, W. C., "Mars Sample Return: Issues and Recommendations," Task Group on Issues in Sample Return, Space Studies Board, National Research Council, National Academy of Sciences, 1997.

[4]Adler, M., "The Mars Sample Return Context for Earth Entry, Descent, and Landing," AIAA Paper 98-2849, June 1998.

[5]Billings, M. D., Fasanella, E. L., and Kellas, S., "Impact Test and Simulation of Energy Absorbing Concepts for Earth Entry Vehicles," AIAA Paper 2001-1602, April 2001.

[6]Young, C. W., "Low Velocity Earth Penetration Study—Wendover Operation," Sandia Labs., Rept. SC-TM-66-2611A, Albuquerque, NM, April 1967.

[7]McCarty, J. L., and Carden, H. D., "Response Characteristics of Impacting Penetrometers Appropriate to Lunar and Planetary Missions," NASA TN D-4454, April 1968.

[8]"MSC.Dytran Version 4.7 User's Manual," Vols. 1 and 2, MSC.Software Corp., Los Angeles, 2000.

[9]Otto, O. R., Laurenson, R. M., Melliere, R. A., and Moore, R. L., "Analyses and Limited Evaluation of Payload and Legged Landing System Structures for the Survivable Soft Landing of Instrumented Payloads," NASA CR-111919, July 1971.

[10]Chen, W. F., "Constitutive Modelling in Soil Mechanics," *Mechanics of Engineering Materials*, edited by C. S. Desai and R. H. Gallagher, Wiley, New York, 1984, pp. 91–120.

[11]Chen, W. F., and Mizuno, E., *Nonlinear Analysis in Soil Mechanics—Theory and Implementation*, Elsevier, Amsterdam, 1990, pp. 263–431.

M. P. Nemeth
Associate Editor